TUNING OF THE FAST LOCAL BUMP SYSTEM FOR HELICITY SWITCHING AT THE PHOTON FACTORY

K. Harada, Y. Kobayashi, T. Miyajima, S. Nagahashi, T. Obina, M. Shimada, R. Takai, KEK-PF, Ibaraki, Japan
S. Matsuba, Hiroshima University, Higashi-Hiroshima, Japan

Abstract

The fast local bump system for helicity switching was installed at a long straight section (B15-B16) at the Photon Factory storage ring in the spring 2008. Recently we have introduced new control system for the fine tuning. In this paper, we present of the system, a tuning method, a demonstration at a slow switching frequency, and a performance at the switching frequency of 10 Hz.

INTRODUCTION

The fast local bump system for helicity switching is expected as a good method to measure the photon helicity-dependence of the material like circular and linear dichroism using a lock-in technique [1]. In order to realize the fast helicity switching, two variably polarizing undulators and five identical bump kickers are going to be installed at a long straight section of 8.9 m at the Photon Factory storage ring (PF-ring). The second undulator will be installed into the ring in this summer.

After the construction of the magnets and the power supplies for the bump system, magnetic field measurements were carried out and then the magnets were installed with the first undulator in the spring 2008. We started the tuning studies of the bump system using the beam, and we succeeded in the orbit switching up to 0.1 Hz with orbit distortion smaller than 10% of beam size outside of the bump and 70 Hz with larger orbit distortion [2].

However, it was impossible to suppress the orbit leakage down to the required values (less than 30 μm in the horizontal direction and 5 μm in the vertical direction) using the previous control system which is consisting of

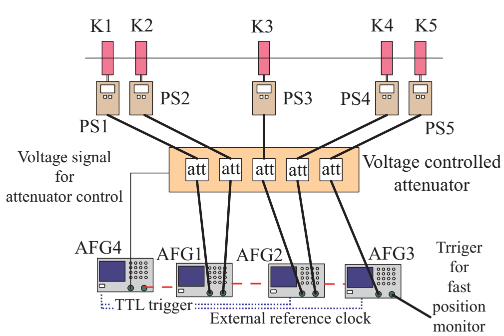

Figure 1: Configuration of the new control system. In this figure, K1~5 are the bump kicker magnets, PS1~5 the power supplies, AFG1~4 the arbitrary function generators. For attenuator, only 5 channels are used and shown in this figure.

#kentaro.harada@kek.jp

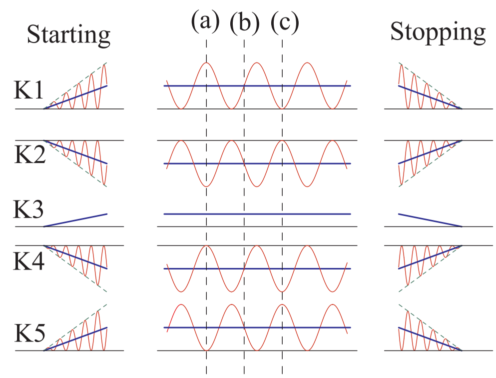

Figure 2: Current waveform for five kickers. Starting operation, the attenuation reduces from 100% to 0%. Stopping operation, it increases from 0% to 100%. The sinusoidal curves show magnetic current waveform consisting of DC offset shown as solid line and AC sinusoidal component. At the timing of (a), the bump height at the upstream insertion device is maximum, and at (c), at the downstream one. At (b), waveform consists of only DC component and this phase is defined as phase origin; $\varphi=2n\pi$ (n : integer). The bump shapes at each case are shown in Fig.3. We note that transverse axes are arbitral for illustration. For usual operation, frequency is fixed through the operation.

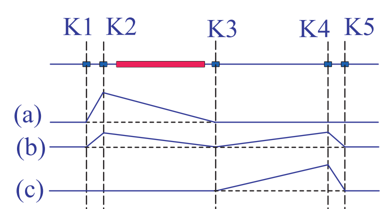

Figure 3: Shape of the bump.

two 4ch DAC (digital analogue converter) modules. Thus, we decided to upgrade the control system since it was difficult to generate completely smooth sinusoidal curve with a high resolution of the amplitude and phase adjustments. Consequently, we introduced four 2ch AFG (arbitrary function generators) modules and voltage-controlled 6ch attenuator modules as new control system in this spring. At the same time, we have developed new tuning methods to use the phase information of the orbit distortion.

NEW CONTROL SYSTEM

Four 2ch AFG modules and voltage-controlled 6ch attenuator modules were adopted for new control system

Table 1: Parameters for Kick Angle Waveform

	K_{DC} [mrad]	K_{AC} [mrad]	δ [rad]	$I_{DC,set}$ [A]	$I_{AC,set}$ [A]
K1	1.15	1.15	0	26.27	26.25
K2	-1.2	1.2	π	-29.94	29.93
K3	0.3			7.59	
K4	-1.2	1.2	0	-29.84	29.84
K5	1.15	1.15	π	26.40	26.39

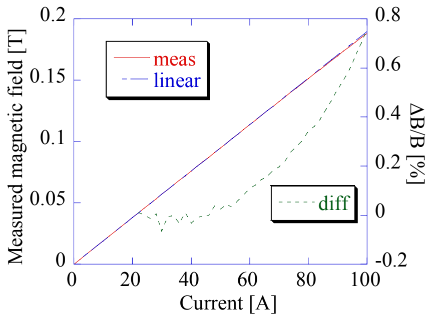

Figure 4: Averaged excitation curve. For the linear part, $B[T] = 0.001897 \cdot I[A]$. The dotted line "diff" shows the difference ratio between measured magnetic field and linear term. The saturation effect seems enough small about current up to about 60 A.

as shown in Fig. 1. In order to produce the local orbit bump with a fast switching, the following kick angle waveform is required for each kicker,

$$\theta_j = K_{DCj} + K_{ACj} \sin(\omega t + \delta_j)$$

where the parameters are listed in Table 1 and kick angle (ie. magnetic current) waveforms are shown in Fig. 2. Bump shape of typical three phases are represented in Fig. 3; phase is $\pi/2+2n\pi$ for (a), $2n\pi$r for (b), $3\pi/2+2n\pi$ for (c) with integer n.

ORBIT DISTORTION SOURCES

Phase and Amplitude Errors

Considering with the errors, the oscillating component of the kick angle can be written by

$$\theta_{AC\,j} = (A_j + \Delta A_j)\sin(\omega t + \delta_j + \Delta\varphi_j),$$

here, ΔA_j is the amplitude error of bump kicker j and $\Delta\varphi_j$ the phase error. Taking the linear and oscillating term of these errors, the error kick is

$$\Delta\theta_{AC\,j} = \Delta A_j \sin(\omega t + \delta_j) + A_j \Delta\varphi_j \cos(\omega t + \delta_j).$$

The orbit distortions from the amplitude error have the same phase as kicker, and those from phase error the phase difference of 90 degrees. In order to realize the tuning of the system, we need to separate these two components by using the phase information.

Resolution of the Control System

For the AFG, voltage can be fixed by 0.001 V step. The voltage control of the power supply is carried out by ±100 A/±10 V. From the magnetic field measurement, it can be

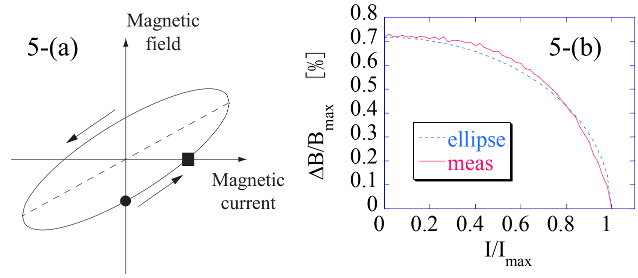

Figure 5: Illustrated typical hysteresis loop. Without hysteresis, the magnetic field is proportional to the current (dotted line in (a)). With hysteresis, the magnetic field follows the trajectory shown as solid line. The difference of magnetic field at quadrant is shown in (b). Approximating this curve by ellipse, the hysteresis effect can be corrected by phase adjustment as to shift "zero phase" from position shown by painted circle to that by painted square in (a).

shown that a magnetic current of 0.01 A generates a kick angle of about 0.4 μrad. For the AFG, the phase can be fixed by about 0.01 degree step (ie. about 170 μrad step). When we take typical amplitude of the kick angle waveform as 1.2 mrad from Table 1, the effective kick angle is corresponding to about 0.2 μrad. From the response matrix of the PF-ring, the ratio of the maximum COD amplitude to error kick angle is about 10. The kick angle of 0.4 μrad generates about 4μm orbit distortion. If we take the permissive beam oscillation amplitude as 1/10 of the beam size, it is typically 30 μm for horizontal direction. Thus the control system allows us to achieve the sufficient resolutions.

Effect of Eddy Current, Saturation and Hysteresis

From the frequency response measurements of the magnets, when the magnetic field is not saturated, the delay of the phase due to the eddy current almost only depends on the frequency. All kickers may have the same delay at a fixed frequency and thus the eddy current have little effect on the orbit distortion.

The averaged excitation curve of the bump kicker is shown in Fig. 4. The maximum magnetic current of the bump system is about 60A and the saturation effect is enough small for this current. When beam energy is increased for 3GeV, however, the magnetic field may be saturated. For such case, even if the magnetic current is ideally sinusoidal waveform of a fixed frequency, the magnetic field has the higher order frequency term;

$$B(I) = cI + c'I^2 \cdots = cI_0 \sin\omega t + c'I_0^2 \sin^2 \omega t \cdots$$

$$= cI_0 \sin\omega t + \frac{c'I_0^2}{2}(1 - \cos 2\omega t) + \cdots.$$

The maximum field of five bump kickers are different and thus the orbit distortions with higher order frequencies may be observed.

The cores of the magnets are made by the silicon steel that has the hysteresis effects. The illustration of the

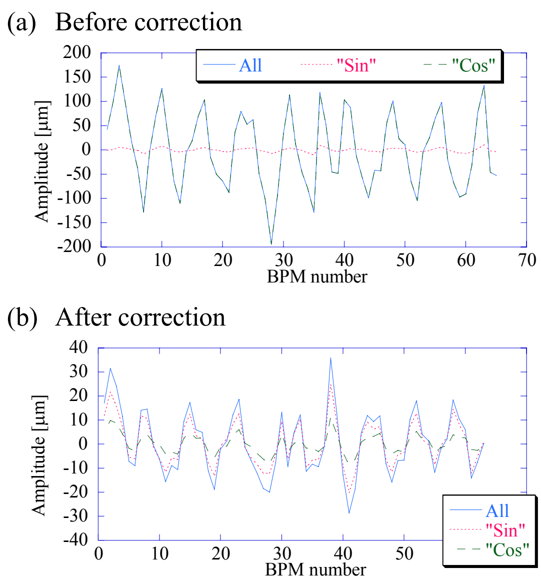

Figure 6: Orbit distortions for slow demonstration.

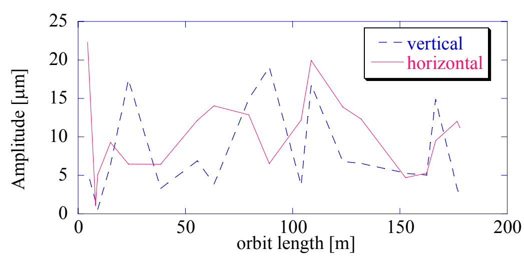

Figure 7: Orbit distortions for 10 Hz operation before tuning.

typical hysteresis loop is shown in Fig. 5. When we approximate the field difference from linear case by ellipse and take the parametric representation, the magnetic field difference due to the hysteresis effect can be written as

$$\begin{cases} I/I_{\max} = \sin \omega t \\ \Delta B/B_{\max} = 0.007 \cos \omega t. \end{cases}$$

When the magnet is sinusoidally excited, the hysteresis effect can be regarded as the magnetic field error that has 90 degree phase difference. Thus the hysteresis effect results in the same kind of orbit distortions as those from the phase errors. By tuning the phase, these distortions can be suppressed.

CORRECTION STRATEGY

Considering the error sources, it seems possible that the orbit distortion can be suppressed to few-microns level that is resolution of AFG. The phase information is essentially important to suppress orbit distortion. The orbit distortion at BPM j can be written as

$$\Delta x_j = \sum_{i=1}^{5} \left(R_{ji} \Delta A_i \sin \varphi + R_{ji} A_i \Delta \varphi_i \cos \varphi \right),$$

here R_{ij} is the orbit response of j-th BPM from the kick by i-th kicker. For the experiment, the measured orbit distortion should be resolved into two parts; "sine" or the amplitude-error component and "cosine" or the phase-error component. For each component, we can calculate the necessary change of the amplitude and the phase by using an ordinary response matrix method.

Because the positions of K1 and K2 are very close, R_{j1} and R_{j2} have almost the same values and R_{j4} and R_{j5} the same. R_{j2} can be written by using R_{j1} as

$$R_{j2} \approx \sqrt{1 + \frac{\Delta\beta}{\beta}} R_{j1} + \widetilde{R}_{j1} \Delta\varphi_{12}$$

here $\Delta\beta$ is difference of beta function and $\Delta\varphi_{12} \approx 0.03$ betatron phase advance between K1 and K2. $\widetilde{R}_{j1}$ is a factor of the same magnitude of R_{j1}. From this expression, difference between R_{j1} and R_{j2} seems about a few %. Thus distortion from K2 can almost be corrected by K1. The tunings of balance of kick angles and relative phase between K1 and K2 are more important than absolute amplitudes and phases of each kicker.

DEMONSTRATION FOR SLOW FREQUENCY CASE

In order to demonstrate the correction method, the bump system is operated and tuned with switching frequency of 250 μHz (one period is about 1 hour). With the usual 65 BPMs, the orbit distortion was measured as shown in Figure 6-(a). It can be seen that the amplitudes are almost optimized and the effects of the phase errors are dominant. After the tuning, the orbit distortion reduced as shown in Figure 6-(b). The new method was successfully demonstrated.

FAST SWITCHING TEST

Finally, 10Hz operation was tested. At present, the measurements of orbit distortions were carried out by eight fast BPMs. With manual cable switching, the orbit distortions from 19 BPM places are measured as shown in Fig. 7. When we change the amplitude of one kicker, the change of the orbit distortion may be observed only in "sine" or amplitude-error component. By using this method, we can set the optimum target of the phase tuning. (In principle, any phase can be fixed as "zero" phase. The iteration of the phase tuning can fix all kickers to "zero" phase.)

In the next beam study, we will try to suppress the orbit distortion for 10Hz case.

REFERENCES

[1] G. Schutz et al., Phys. Rev. Lett. 58, (1987) 737.
[2] S. Matsuba et al., Proc. of PAC09, (2009).